

Learned reconstruction with convergence guarantees

Subhadip Mukherjee^{*1}, Andreas Hauptmann^{*2,3}, Ozan Öktem⁴, Marcelo Pereyra⁵, and Carola-Bibiane Schönlieb¹

¹University of Cambridge, UK; ²University of Oulu, Finland; ³University College London, UK;

³KTH–Royal Institute of Technology, Sweden; ⁴Maxwell Institute for Mathematical Sciences & Heriot-Watt University, UK; ^{*}Equal contribution

E-mails: andreas.hauptmann@oulu.fi, sm2467@cam.ac.uk, ozan@kth.se, m.pereyra@hw.ac.uk, cbs31@cam.ac.uk

Abstract

In recent years, deep learning has achieved remarkable empirical success for image reconstruction. This has catalyzed an ongoing quest for precise characterization of correctness and reliability of data-driven methods in critical use-cases, for instance in medical imaging. Notwithstanding the excellent performance and efficacy of deep learning-based methods, concerns have been raised regarding their stability, or lack thereof, with serious practical implications. Significant advances have been made in recent years to unravel the inner workings of data-driven image recovery methods, challenging their widely perceived black-box nature. In this article, we will specify relevant notions of convergence for data-driven image reconstruction, which will form the basis of a survey of learned methods with mathematically rigorous reconstruction guarantees. An example that is highlighted is the role of input-convex neural networks (ICNNs), offering the possibility to combine the power of deep learning with classical convex regularization theory for devising methods that are provably convergent.

This survey article is aimed at both methodological researchers seeking to advance the frontiers of our understanding of data-driven image reconstruction methods as well as practitioners, by providing an accessible description of convergence concepts and by placing some of the existing empirical practices on a solid mathematical foundation.

Index Terms

Inverse problems, data-driven regularization, convexity, proximal operators, Bayesian methods.

I. INTRODUCTION

Image reconstruction problems are virtually ubiquitous in scientific and engineering applications; ranging from astronomy to clinical diagnosis, from electron microscopy to X-ray crystallography. In such problems, an image of interest needs to be recovered from its incomplete and noisy observation. The data generation process is governed by an underlying physical process, precise knowledge of which is a prerequisite to formulate a reconstruction problem.

It is of paramount importance, especially for critical use-cases such as medical imaging, to obtain image reconstructions with reliable content as they contain critical structural information about the object of interest. Moreover, in many applications of computational imaging, image reconstruction is used as a tool for scientific discovery without any ground-truth being available. Therefore, one needs to be able to rely on the correctness of the reconstruction result. Correctness and reliability of reconstruction algorithms have been traditionally provided in terms of convergence guarantees, and more specifically, in the framework of model-based variational regularization [1]. Mathematically, image reconstruction is an example of an inverse problem, where research is primarily concerned with the development and analysis of mathematical theory and algorithms in a fairly general setting. Such guarantees also offer a principled framework for practitioners to control the reconstruction process.

The emergence of deep learning and the availability of high-quality training data have considerably transformed the research landscape of image reconstruction and attracted a significant amount of attention in recent years [2]. Image quality has improved to a considerable extent as compared to the classical model-based techniques, both qualitatively and quantitatively, driven by task-specific image data sets and sophisticated machine learning algorithms. Some concerns have been voiced nevertheless, pointing out the lack of adequate comprehension of what happens within the learned reconstruction methods, putting forward the argument that a more thorough understanding is needed for reliable utilization of these techniques. Consequently, in parallel with the ongoing enterprise of designing more efficient and better-performing data-driven reconstruction approaches, researchers have begun to investigate theoretical properties of these methods for image reconstruction.

A specific question is whether one can provide reconstruction guarantees and convergence results for deep learning-based methods. This question is important to theoreticians and practitioners alike, since successful answers would place empirically successful methods, often based on heuristics, on a rigorous theoretical foundation. Nevertheless, the notion of *theoretical guarantees* is imprecise and can have different meanings depending on the specific context.

This survey attempts to define different notions of convergence within the realm of image reconstruction, elaborate on their practical implications, and present an overview of recent deep learning-based image reconstruction methods that fit into the different notions of convergence. We argue that many of the recently proposed deep learning-based approaches come with more theoretical backing than it is often communicated and are, in fact, not as much a black-box as they are generally referred to be. In particular, identifying the connections between model- and data-driven methods will help unite the two seemingly disparate paradigms and broaden our knowledge of this exciting new line of research.

The article is organized as follows. In Sec. II, we provide the mathematical preliminaries for inverse problems and explain different training strategies for data-driven image reconstruction. This section facilitates precise characterization of different convergence notions, which appears in Sec. III, in a

rigorous yet accessible manner. The ideas of convergence considered in this article are primarily derived from the classical regularization, convex analysis, and statistics literature. Sec. IV provides a review of recent notable data-driven methods that come with convergence guarantees introduced in the preceding section. Our survey is not exhaustive by any means, in that it excludes approaches that are based on heuristics and are not provably convergent (except for a few pioneering methods that inspired new lines of research). It is also worth emphasizing that the methods chosen for review are not necessarily the best-performing methods empirically, but they are more interpretable in the classical sense and hence more transparent as compared to competing techniques with possibly superior numerical performance. Finally, we present a summary and make some concluding remarks in Sec. V.

II. MATHEMATICAL FOUNDATIONS

In order to characterize what convergence and reconstruction guarantees mean for an image reconstruction problem, we need to mathematically formulate the reconstruction task.

In the traditional deterministic *functional analytical* setting, this is viewed as solving an operator equation. More precisely, one seeks to find $x^* \in \mathbb{X}$, which is unknown but deterministic, from measured data $y \in \mathbb{Y}$ under the measurement model $y = \mathcal{A}x^* + e$, where $e \in \mathbb{Y}$ denotes observation error. Here, $\mathcal{A}: \mathbb{X} \rightarrow \mathbb{Y}$ (*forward operator*) models how an image gives rise to data in the absence of observation error and is typically derived from a careful modeling of the involved physics. In particular, we concentrate here on linear operators \mathcal{A} that can be represented by a matrix for discretized images. The spaces \mathbb{X} and \mathbb{Y} can be fairly general and potentially infinite-dimensional function spaces, however for the purpose of our exposition, it suffices to consider them as finite-dimensional vector spaces endowed with an inner-product and norm (in particular, subsets of Euclidean spaces).

Bayesian inversion extends the above by introducing an \mathbb{X} -valued random variable \mathbb{x} that generates the true (unknown) image $x^* \in \mathbb{X}$ and the distribution (prior) of \mathbb{x} serves as a statistical model for images in \mathbb{X} . Then, image reconstruction becomes a statistical inference task where measured data $y \in \mathbb{Y}$ is a single sample of a \mathbb{Y} -valued (conditional) random variable ($y|\mathbb{x} = x^*$), where $x^* \in \mathbb{X}$ is the true (unknown) image and $y = \mathcal{A}\mathbb{x} + \mathbb{e}$, for some \mathbb{Y} -valued random variable \mathbb{e} . Here, \mathbb{x} is an \mathbb{X} -valued random variable that generates the true (unknown) signal x^* and whose marginal distribution (prior) constitutes a statistical model for images. The desired image can now be recovered by formulating a *reconstruction method*, represented by a mapping $\mathcal{R}: \mathbb{Y} \rightarrow \mathbb{X}$. In the functional analytic setting, this corresponds to a regularized inverse of \mathcal{A} , whereas in Bayesian inversion, it represents to an estimator that summarizes the posterior distribution of the \mathbb{X} -valued random variable ($\mathbb{x}|y = y$). A key challenge is to handle the *ill-posedness* of inversion, which arises from the fact that the forward operator \mathcal{A} in practical inverse problems is either under-determined or poorly-conditioned with an unstable inverse. This leads to non-uniqueness and instability of reconstruction, meaning that many

candidate images explain the measured data even in the absence of noise, or a small amount of noise in the data results in large changes in the recovered image. One can circumvent ill-posedness by introducing a *regularization* to stabilize the reconstruction, for instance by enforcing certain regularity conditions, such as smoothness. In Bayesian inversion, regularization is often achieved by selecting a prior distribution on images, which assigns low likelihood to images with unwanted features. In both settings, regularization involves a handcrafted a model that encodes prior knowledge as well as expected properties of the solution.

A. Model-based reconstruction

The design of regularized reconstruction methods is traditionally based on the functional analytic view. Early approaches sought to provide an analytic pseudo inverse to the forward operator (*direct regularization*). An example is the filtered back-projection (FBP) method for tomographic image reconstruction, which regularizes by recovering the band-limited part of the image. A drawback of such an approach is that it is problem-specific, and does not generalize to a different forward operator.

Thus, it is desirable to formulate a general class of reconstruction methods that allow to replace the forward operator in a plug-and-play manner. This leads to *variational models*, where the reconstruction task is formulated as a minimization problem of some penalty function $\mathcal{J}: \mathbb{X} \times \mathbb{Y} \rightarrow \mathbb{R}$ that ensures data-consistency and incorporates a regularizer. More precisely, such a penalty function typically takes the form $\mathcal{J}(x, y) := \mathcal{L}_{\mathbb{Y}}(\mathcal{A}x, y) + \mathcal{S}_{\vartheta}(x)$, where $\mathcal{L}_{\mathbb{Y}}: \mathbb{Y} \times \mathbb{Y} \rightarrow \mathbb{R}$ quantifies consistency in data space \mathbb{Y} and the regularizer $\mathcal{S}_{\vartheta}: \mathbb{X} \rightarrow \mathbb{R}$ penalizes undesirable solutions. The data consistency term is often taken to be the least-squares loss $\mathcal{L}_{\mathbb{Y}}(\mathcal{A}x, y) := \|\mathcal{A}x - y\|_2^2$, which, if minimized without regularization, leads to overfitting the measurement noise. This underlines the need of including a regularization term \mathcal{S}_{ϑ} with possible hyper-parameters $\vartheta \in \mathbb{R}^d$, which allows to encode prior knowledge about expected solutions, such as sparsity assumptions [1]. The reconstruction method $\mathcal{R}_{\vartheta}: \mathbb{Y} \rightarrow \mathbb{X}$ with $\vartheta \in \mathbb{R}^d$ is now defined as the solution operator for the minimization problem

$$\mathcal{R}_{\vartheta}(y) \in \arg \min_{x \in \mathbb{X}} \mathcal{J}_{\vartheta}(x, y) \quad \text{where} \quad \mathcal{J}_{\vartheta}(x, y) := \mathcal{L}_{\mathbb{Y}}(\mathcal{A}x, y) + \mathcal{S}_{\vartheta}(x). \quad (1)$$

The hyper-parameter ϑ needs to be chosen beforehand depending on the noise level in the data. Solutions to (1) are then often computed through an *iterative scheme* by (proximal) gradient-based methods, which are the basis for the unrolling techniques discussed in Sec. IV.

Some of the above methods can be interpreted as Bayes estimators. If the data-discrepancy $\mathcal{L}_{\mathbb{Y}}(\mathcal{A}x, y)$ is proportional to the negative log-likelihood for $(y|x = x)$, then minimizing it corresponds to maximum-likelihood estimation. In addition, if the regularizer $\mathcal{S}_{\vartheta}(x)$ in (1) is proportional to the negative log-prior density of \mathbb{X} , then (1) can be interpreted as maximum a-posteriori probability (MAP) estimation [3].

B. Data driven reconstruction

Although model-based inversion such as variational models with highly complex and sophisticated analytical regularizers represent a promising approach to solve ill-posed inverse problems, they pose two key challenges: (i) *handcrafting* a sufficiently expressive regularizer (or prior) and (ii) ensuring computational feasibility of hyper-parameter selection and evaluation. These challenges are more pronounced for Bayesian inversion. Algorithms to approximate the posterior mean and for uncertainty quantification are typically based on Markov chain Monte Carlo (MCMC) methods, which require carefully constructed priors and tend to be computationally infeasible for time-critical applications.

The development of data-driven reconstruction is inspired by the need to address the above challenges of achieving computational feasibility and selection of a domain adapted regularizer/prior. Instead of handcrafting a reconstruction method, data-driven methods use training data to learn an *optimal* reconstruction method based on statistical learning. We will focus here on (*learned reconstruction*) methods $\mathcal{R}_\theta: \mathbb{Y} \rightarrow \mathbb{X}$ that are typically parametrised by some suitably chosen deep neural network (DNN) and thus learning refers to selecting optimal parameters $\hat{\theta}$ from the training data. This, however, depends on the statistical properties of the training data as discussed in the following and, as we will see later, has an effect on the type of convergence we obtain.

a) Supervised learning: In this case, one has access to pairs of ground-truth images and corresponding measurements following the measurement model $y = \mathcal{A}x + e$. That is, training data are given as i.i.d. samples $(x_1, y_1) \dots, (x_n, y_n) \in \mathbb{X} \times \mathbb{Y}$ of (\mathbb{x}, \mathbb{y}) . An optimal set of parameters $\hat{\theta}$ for the reconstruction method is found by empirical risk minimization given a suitable loss function $\mathcal{L}_{\mathbb{X}}: \mathbb{X} \times \mathbb{X} \rightarrow \mathbb{R}$ in the image domain:

$$\hat{\theta} \in \arg \min_{\theta} \frac{1}{n} \sum_{i=1}^n \mathcal{L}_{\mathbb{X}}(\mathcal{R}_\theta(y_i), x_i). \quad (2)$$

Usual choices for the loss function include the squared ℓ^2 -norm, where $\mathcal{L}_{\mathbb{X}}(x, x') := \|x - x'\|_2^2$.

The formulation in (2) does not explicitly include the forward operator, or more generally, the data likelihood. Nevertheless, this is implicitly incorporated by the choice of training data that satisfy $y_i \approx \mathcal{A}x_i$. One can now select a parametrization $\mathcal{R}_\theta: \mathbb{Y} \rightarrow \mathbb{X}$ that accounts for the fact that a trained estimator should represent a regularized inversion method. A popular example of such a domain-adapted parametrization is to combine a DNN $\mathcal{C}_\theta: \mathbb{X} \rightarrow \mathbb{X}$ with a handcrafted pseudo inverse $\mathcal{A}^\dagger: \mathbb{Y} \rightarrow \mathbb{X}$, which incorporates a direct regularization, as discussed in Sec. II-A. The learned reconstruction operator is then represented by the composition $\mathcal{R}_\theta := \mathcal{C}_\theta \circ \mathcal{A}^\dagger$ where $\mathcal{C}_\theta: \mathbb{X} \rightarrow \mathbb{X}$ acts as a learned post-processing operator that removes noise and under-sampling artifacts. Popular architectures in imaging are based on convolutional neural networks (CNNs), more specifically convolutional autoencoders with an encoding/decoding branch, such as the popular U-Net [4] and related architectures inspired by harmonic analysis [5]. The supervised setting applies to the case where pairs of high- and low-quality

reconstructions are available, such as low-dose and high-dose computed tomography (CT) scans. In this case, the high-dose reconstruction can be identified with x and the low-dose measurements provides the data y to obtain an initial reconstruction by applying the pseudo-inverse operator \mathcal{A}^\dagger , which can be considered a pre-computation step before the training procedure.

Another highly popular parametrization for \mathcal{R}_θ is based on so-called *unrolling*. The idea is to start with some iterative scheme, like one designed to minimize $x \mapsto \mathcal{L}_\mathbb{Y}(\mathcal{A}x, y)$ or the objective in (1). Next, the iterative scheme is truncated to a fixed number of iterations and unrolled by replacing selected handcrafted updates with (possibly shallow) neural networks (NNs). Notably, for model-based learning, one does not usually replace \mathcal{A} and its adjoint \mathcal{A}^\top , but other components such as the proximal operator [2, Sec. 4.9.1]. Hence, the DNN for \mathcal{R}_θ is formed by combining (shallow) NNs with physics-driven operators. Popular examples of unrolled networks include learned primal-dual [6], and variational networks [7]. At this point, we would like to stress that *unrolling is merely a way to select an architecture for the DNN parametrizing \mathcal{R}_θ* . In particular, training as in (2) does *not* yield a solution operator for (1) even if the DNN is constructed by unrolling an optimization solver.

b) Unsupervised learning: This type of learning comes in two flavors, depending on whether high-quality images or measurement data are available. In the former case, training data $x_1, \dots, x_n \in \mathbb{X}$ are i.i.d. samples of \mathfrak{x} . One can then consider reconstruction methods \mathcal{R}_θ of the form in (1) with a regularizer/prior $\mathcal{S}_\theta: \mathbb{X} \rightarrow \mathbb{R}$ (here $\theta = \vartheta$) that is learned from training data through generative modeling, like generative adversarial networks (GANs) or variational auto-encoders (VAEs). GAN-based approaches implicitly regularize the reconstruction by restricting it to the range of a pre-trained generator [8], whereas the other alternative is to learn an explicit regularizer parametrized by a DNN [9], [10].

The other variant is when training data $y_1, \dots, y_n \in \mathbb{Y}$ are i.i.d. samples of \mathfrak{y} . One option is to learn a data driven solver for optimization problems of the type in (1) where the objective is parameterized by $y \in \mathbb{Y}$ (see [11] for further details). In this setting, it is quite natural to parametrize \mathcal{R}_θ by a DNN whose architecture is given by unrolling an optimization solver for (1). Hence, contrary to the supervised setting above, the trained DNN approximates the solution for the minimization in (1).

c) Weakly supervised learning: This refers to the case where samples of measurement data and ground-truth are available, but they are not paired. Training data then consists of un-paired $x_1, \dots, x_n \in \mathbb{X}$ and $y_1, \dots, y_n \in \mathbb{Y}$ in the sense that $x_i \in \mathbb{X}$ and $y_i \in \mathbb{Y}$ are i.i.d. samples of the \mathfrak{x} - and \mathfrak{y} -marginal distributions of $(\mathfrak{x}, \mathfrak{y})$, respectively. Such data can be used to set-up a learning problem which quantifies consistency against data and image error similar to (2), but using loss-functions on both \mathbb{X} and \mathbb{Y} . This is complemented with a term that quantifies similarity of probability distributions induced by training data, thus resulting in an elaborate learning problem, see [2, eq. (5.3)]. The learning problem is recast into a more suitable form by using deep generative models.

Notable methods that fall within the weakly supervised training paradigm are adversarial regularizer

(AR) [10] and its convex variant given by adversarial convex regularizer (ACR) [12]. Both of these seek to learn a regularizer in a variational model as a critic that can tell apart noisy reconstructions (obtained through some simple baseline approach, e.g., by applying the pseudo-inverse of \mathcal{A} on the measurements) from the ground-truth image samples x_i . The regularizer is restricted to be Lipschitz-continuous (and convex in case of ACR), which plays an important role in the stability analysis of the resulting variational model. Lipschitz-continuity of the regularizer is enforced via a soft-penalty (see [10], [12] and references therein), whereas convexity is enforced by the choice of DNN architecture.

III. TYPES OF CONVERGENCE

Now that we have established the concept of reconstruction methods, regularization, and learned reconstruction, the question that remains is: what are the theoretically desired properties of a learned reconstruction? For instance, if we think about iterative reconstruction, the question of convergence is relevant. Does the iterative scheme converge to a fixed point? Does this fixed point correspond to a minimizer of a variational loss, such as in (1)? Moreover, is it, in fact, a regularization method? These are not only purely academical questions, but provide interpretability and guarantees of correctness of the obtained solution. The following section aims to outline important notions of convergence that are relevant for the image reconstruction task at hand in an accessible way, while not compromising on the mathematical rigor.

a) Formal stability: The weakest and arguably the most fundamental mathematical guarantee comes in the form of *stability*, which has its origin in Hadamard’s definition of well-posedness [1]. *Stability* refers to a smooth variation of the reconstruction with respect to changes in the observed data (see box). The notion of stability can also be applied to Bayesian inversion, in which case it refers to the stability of posterior probabilities, statistical moments, and/or Bayesian estimators. When we refer to provable stability in the following, we mean that it is possible to estimate and control the maximal error in the reconstruction with respect to deviations in the measurement (for instance, in terms of the Lipschitz constant). It should be also noted, that the notion of stability (or lack thereof) itself can be quite meaningless, if no further conditions are provided. For instance, a reconstruction method that always produces the same image from varying data is in fact stable, but useless in practice.

Stability versus adversarial stability

Consider a trained reconstruction operator \mathcal{R}_θ with fixed network parameters. One possibility for a stability analysis is to consider the Lipschitz constant L of the mapping \mathcal{R}_θ , which is given by the smallest $L > 0$, such that

$$\|\mathcal{R}_\theta(y_1) - \mathcal{R}_\theta(y_2)\| \leq L\|y_1 - y_2\|, \quad (3)$$

for all $y_1, y_2 \in \mathbb{Y}$. Thus, L controls the maximal deviation between reconstructions corresponding

to two observations y_1 and y_2 . Since DNNs are compositions of affine functions and smoothly varying nonlinear activations, a mapping \mathcal{R}_θ modeled using DNNs is continuous and a constant L satisfying (3) exists. However, although \mathcal{R}_θ is formally stable, the constant L might be large, leading to large deviations in the reconstruction for small changes in the measurement. This is where the concept of adversarial stability comes into the picture as an attempt to find the worst-case scenario. The idea in adversarial stability is to find the smallest perturbation that causes the largest error, for instance, by solving: $\min_{z \in \mathbb{Y}} \beta \|z\| - \|\mathcal{R}_\theta(y) - \mathcal{R}_\theta(y+z)\|$. Such an analysis can be performed for any reconstruction method, like classical compressed sensing methods that equally exhibit adversarial vulnerability for a fixed regularization parameter [13].

b) *Fixed-point convergence*: To solve a reconstruction problem iteratively starting from an initial guess, one applies an operator updating $\mathcal{T}: \mathbb{X} \rightarrow \mathbb{X}$ on the previous iterate(s): $x_{k+1} := \mathcal{T}(x_k)$. The operator \mathcal{T} typically involves the forward operator, its adjoint, and the observed data. It is important to determine whether iterates converge. One such notion is *fixed-point convergence*, which means that $\lim_{k \rightarrow \infty} x_k = x_\infty$, where $x_\infty := \mathcal{T}(x_\infty)$ is a fixed-point of \mathcal{T} . If fixed-point convergence holds, the iterates stabilize after sufficiently many steps, which is clearly desirable for an iterative scheme. However, it does not necessarily tell anything about what kind of solutions the iteration converges to.

c) *Convergence to the minimum of a variational loss (objective convergence)*: For a stronger notion of convergence of an iterative algorithm, one can consider minimizing a variational loss, similar to (1). That is, we consider the loss function of the form $\mathcal{J}(x) := \mathcal{L}_{\mathbb{Y}}(\mathcal{A}x, y) + \lambda \mathcal{S}_\vartheta(x)$ for data $y \in \mathbb{Y}$. In an optimization algorithm, an initial guess is refined iteratively by exploiting, for instance, information about the gradient $\nabla \mathcal{J}$ at each step to compute a minimizer. Such an iterative scheme $x_{k+1} := \psi_{\theta_k}(x_k, \nabla \mathcal{J}(x_k))$ with an updating rule $\psi_\theta: \mathbb{X} \times \mathbb{X} \rightarrow \mathbb{X}$ and iteration-dependent parameters $\theta := \{\theta_1, \theta_2, \dots\}$ is said to converge to a minimizer if $x_k \rightarrow \arg \min_{x \in \mathbb{X}} \mathcal{J}(x)$ as $k \rightarrow \infty$. That is, we can now characterize the point of convergence as the minimizer of an objective function. We will refer to this notion of convergence as *objective convergence* in the remainder of the paper.

d) *Convergent regularization*: The strongest form of convergence we discuss here considers whether a regularized solution for an ill-posed inverse problem with (linear) forward operator $\mathcal{A}: \mathbb{X} \rightarrow \mathbb{Y}$ tends to the corresponding solution $y^0 \in \mathbb{Y}$ obtained from noise-free data as the noise level vanishes. This could be viewed as a second level of convergence, as convergence of the iterative scheme is needed.

Formally, a regularization method can be understood as a parameterized family $\{\mathcal{R}_\vartheta\}_{\vartheta \in \mathbb{R}^d}$ of reconstruction methods. Here, the parameter ϑ depends on the noise level $\delta > 0$, where $\|y^\delta - y^0\| \leq \delta$ with $y^0 := \mathcal{A}x^*$ denoting noise-free data. A regularization method is convergent if there exists a parameter choice rule $\delta \mapsto \vartheta(\delta, y^\delta)$ such that reconstructions converge to a pseudo-inverse solution as noise vanishes, i.e., $\mathcal{R}_{\vartheta(\delta, y^\delta)}(y^\delta) \rightarrow \mathcal{A}^\dagger(y^0)$ as $\delta \rightarrow 0$.

In the context of variational models (1), one can re-formulate the above as follows: Let $x_{\vartheta, \delta} \in \mathbb{X}$ denote

a minimizer to the objective in (1) for given ϑ and data $y^\delta \in \mathbb{Y}$ with noise level $\|e\| = \|y - y^0\| < \delta$. Next, assume also that there is a parameter choice rule $\delta \mapsto \vartheta(\delta, y^\delta)$. The variational model defined by (1) is said to *converge to an \mathcal{S} -minimizing solution* if $x_{\vartheta(\delta, y^\delta), \delta} \rightarrow x^\dagger$ as $\delta \rightarrow 0$. Here, $x^\dagger \in \mathbb{X}$ solves the variational model that corresponds (1) with noise-free data $y^0 \in \mathbb{Y}$, i.e.,

$$x^\dagger \in \arg \min_{x \in \mathbb{X}} \mathcal{S}_{\vartheta_0}(x) \quad \text{subject to } y^0 = \mathcal{A}x \text{ and where } \vartheta_0 := \lim_{\delta \rightarrow 0} \vartheta(\delta, y^\delta). \quad (4)$$

Fig. 1 shows such convergence in the context of ACR [12], a learned convex regularizer.

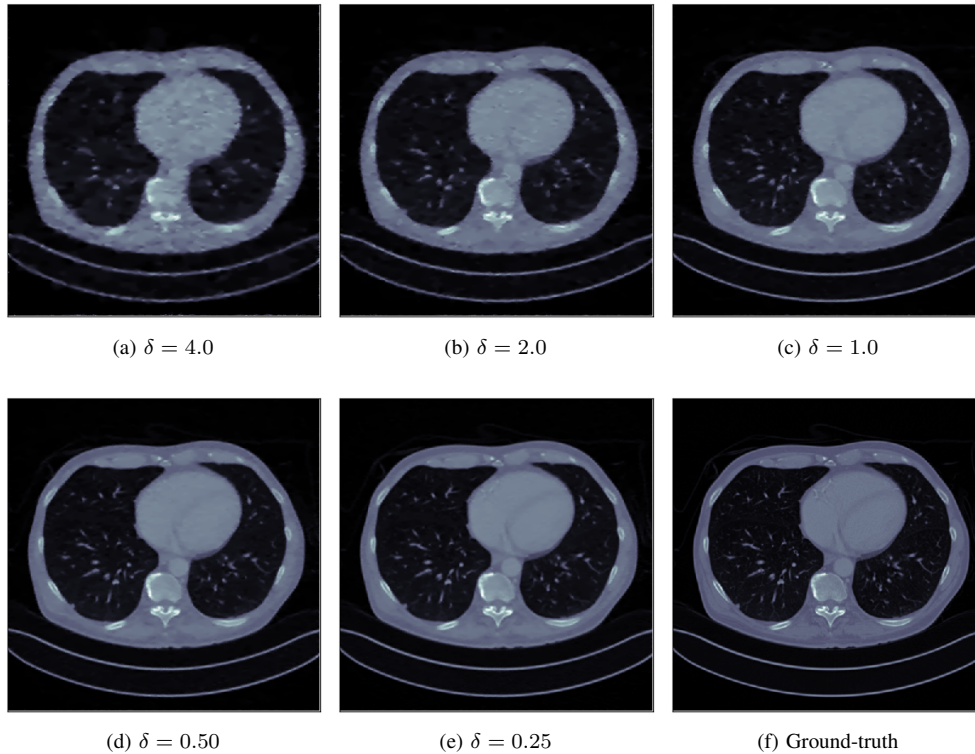


Fig. 1: ACR [12] as a convergent regularization strategy: The reconstructed image converges to the ground-truth as $\delta \rightarrow 0$, subject to an appropriate parameter choice rule for the scalar regularization parameter: $\delta \mapsto \lambda(\delta) > 0$. Here, the regularizer parameter ϑ is learned from data and kept fixed during reconstruction.

e) Convergence for Bayesian inversion: The concept of convergence in the Bayesian setting concerns distance between probability distributions. For instance, the convergence properties of iterative stochastic sampling methods for general Bayesian computation are often studied by establishing that the probability distribution of the generated Monte Carlo (MC) samples contracts towards a target distribution of interest in some suitable probability metric. The strongest convergence results in this context are derived from the total variation (TV) metric, which implies the convergence of probabilities. Alternatively, many works study convergence in a Wasserstein metric of order p , which guarantees weak convergence (pertaining to expectations of bounded continuous functions, but not probabilities), plus convergence of the first p moments (see [14] for other metrics and their relationships).

Special attention is paid to the rate of the contraction towards the target distribution. It is desirable

that the distance to the target decreases geometrically fast with respect to the number of iterations, as this guarantees an efficient exploration of the space and the correct behavior of Monte Carlo estimators (these estimators can behave poorly if the algorithm converges too slowly). Works on the topic often seek to also characterize the dependence of the contraction rate on various key aspects of the problem (e.g., dimension, conditioning, tail behavior, and initialization), as well as to establish if the algorithm converges exactly or with asymptotic bias (i.e., to a neighborhood of the target). While conventional Bayesian computation approaches are asymptotically unbiased, modern large-scale strategies often accept some bias to achieve significantly faster convergence rates.

The convergence of deterministic iterative Bayesian computation methods, such as variational Bayes and approximate message passing (AMP), is studied by using techniques that are broadly similar to the ones used to study optimization algorithms (with some results holding in the large system limit). For MAP estimation, convergence is formulated as a contraction towards a critical point of the density function, or a neighborhood of the set of critical points in the case of algorithms with bias.

Convergence issues aside, recent theory on Bayesian inference with data-driven priors focuses on proving existence and stability of the associated posterior distributions with respect to perturbations in the observed data, as well as the existence and stability of the probabilities, moments, and estimators that the algorithms seek to compute.

IV. PROVABLE STABILITY AND CONVERGENCE

Most learned reconstruction methods $\mathcal{R}_\theta: \mathbb{Y} \rightarrow \mathbb{X}$ are formally stable since they are continuous mappings. This is the case with one-step methods $\mathcal{R}_\theta := \mathcal{C}_\theta \circ \mathcal{A}^\dagger$ whenever the pseudo inverse $\mathcal{A}^\dagger: \mathbb{Y} \rightarrow \mathbb{X}$ and the learned post-processor $\mathcal{C}_\theta: \mathbb{X} \rightarrow \mathbb{X}$ are continuous. Likewise, common unrolling architectures for \mathcal{R}_θ , like variational networks [7] and learned primal-dual (LPD) [6], are continuous. The above claims are supported by Fig. 2, which shows performance of FBPconvNet (one-step method) and LPD (unrolling architecture). In contrast, a reconstruction operator given by a variational scheme with a learned regularizer, as in AR, is not necessarily continuous. Further, even if the reconstruction operator is formally continuous, its Lipschitz constant can be large, resulting in loose stability bounds.

Regarding convergence, most results can be placed within the variational framework with either an explicit or an implicit regularizer, see Fig. 3 for an overview the discussed methods. Explicit regularization schemes model the regularizer directly through a neural network, whereas the implicit schemes regularize the solution via a denoiser (also known as plug-and-play methods). The explicit regularization schemes [10], [9], [12] typically come with a stability or convergent regularization guarantees, whereas the plug-and-play methods have been shown to possess either fixed-point or objective convergence subject to different constraints on the denoiser.

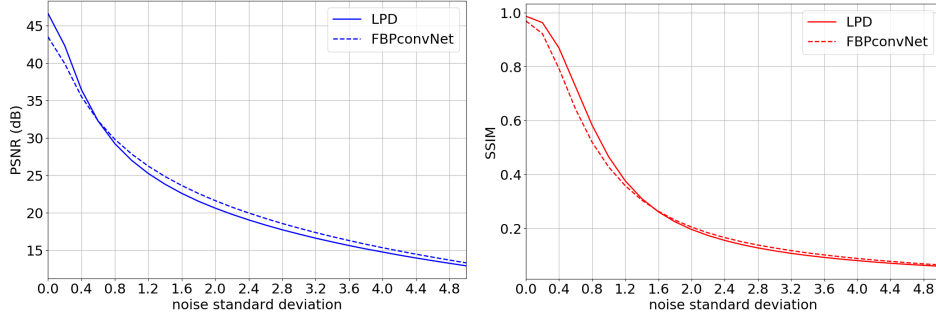


Fig. 2: Reconstruction quality (PSNR left and SSIM right) as a function of noise level in data for LPD (unrolling) [6] and FBPconvNet (one-step) [4] methods. Both methods are trained against simulated noise-free 2D CT data generated from 2D images that are cross sections of anthropomorphic phantoms in the AAPM low-dose CT challenge.

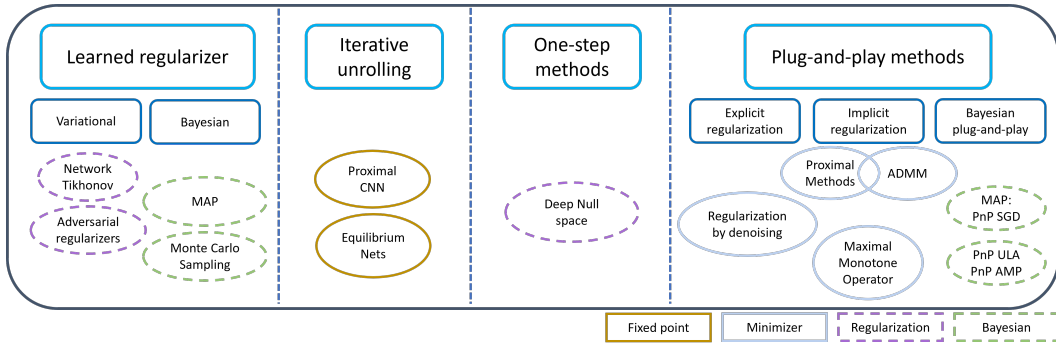


Fig. 3: Categorization of data driven reconstruction methods, which are color-coded based on the strongest type of convergence guarantee they satisfy.

A. Learned regularization methods

These methods are based on learning a DNN representing a regularizer $\mathcal{S}_\vartheta: \mathbb{X} \rightarrow \mathbb{R}$ in a variational model of the form (1) (learned regularizer) or reconstruction by considering images generated by a DNN (regularization-by-architecture).

Inspired by the optimal transport theory, an adversarial framework for learning the regularizer was proposed in [10]. This method, also referred to as the adversarial regularizer (AR) method, comes with stability guarantees subject to the regularizer being 1-Lipschitz and coercive. Its convex counterpart (abbreviated as ACR) models the regularizer using an ICNN [15]. The analysis of ACR [12] follows from the classical convex regularization theory and one can formally establish well-posedness of the reconstruction problem (i.e., existence and uniqueness of the solution, and its continuous dependence on the observed data) using (strong) convexity of the regularizer. Moreover, ACR can be shown to be a convergent regularization technique using function-analytic tools in classical regularization theory for inverse problems. Another approach to learning a regularizer is the network Tikhonov (NETT) method [9], which considers a learned regularizer given by a CNN that is trained using an encoder-decoder set-up. The resulting variational model is shown to be well-posed and convergent subject to mild conditions (see [9, Condition 2.2]) on the neural network that parametrizes the regularizer. Other

variants and extensions of NETT (such as augmented NETT and the synthesis counterpart of NETT) are also provably convergent regularization methods.

A slightly different approach is [16], which can be seen as a regularization-by-architecture scheme akin to deep image prior [17]. Regularization properties for this method are shown rigorously by constructing the generator as a multi-level sparse coding network. The approach proposed in [18] is similar in spirit with [16], in the sense that regularization is achieved by restricting the image to lie in the range of an untrained generator network. The paper provides recovery guarantees that are similar to the compressed sensing guarantees in flavor (using the so-called set-restricted eigenvalue condition). This condition is essentially same as the restricted isometry condition, but defined for all images in the range of the generator. In contrast with [17], [18], the method developed in [19] seeks a reconstruction in the range of a pre-trained generator. A proximal gradient-descent (PGD) algorithm is used for recovery by replacing the projection operator on to the range of the generator with a learned network. The recovery algorithm is provably convergent.

Adversarial regularizers: Why convexity matters

Consider a denoising problem on the real line^a (i.e., $\mathbb{X} = \mathbb{R}$), where the distribution of ground-truth is given by $p^*(x) = \frac{1}{2}(\delta_{-1}(x) + \delta_1(x))$, two Dirac pulses at $+1$ and -1 . Let the noisy data have distribution $p_{\text{noisy}} = U([- \frac{1}{2}, \frac{1}{2}])$, uniform distribution over $[- \frac{1}{2}, \frac{1}{2}]$. Recall the adversarial learning framework [10], wherein the regularizer is trained to discern the distribution of the ground-truth from that of some baseline reconstruction: $\min_{\mathcal{S} \in \text{Lip}(\mathbb{X})} \mathbb{E}_{\mathbb{x} \sim p^*} \mathcal{S}(\mathbb{x}) - \mathbb{E}_{\mathbb{x} \sim p_{\text{noisy}}} \mathcal{S}(\mathbb{x})$, where $\text{Lip}(\mathbb{X})$ is 1-Lipschitz functionals on \mathbb{X} . The optimal regularizer in this case turns out to be $\mathcal{S}^*(x) = 1 - |x|$ and the resulting variational problem for denoising reads as

$$\min_x \frac{1}{2}(x - y)^2 - \lambda|x|, \quad \text{where } 0 < \lambda < \frac{1}{2}. \quad (5)$$

One can solve (5) in closed form as

$$\hat{x}(y) = \begin{cases} y + \lambda & \text{for } y \geq 0 \\ y - \lambda & \text{for } y < 0. \end{cases} \quad (6)$$

Clearly, the reconstruction given by (6) changes drastically as the data y changes sign and is therefore discontinuous at $y = 0$. Note that it does not violate the stability guarantee of AR, which only ensures convergence up to sub-sequences. For instance, consider a sequence $y_k = (-1)^k \frac{1}{k}$ for $k = 1, 2, \dots$, so $y_k \rightarrow 0$ as $k \rightarrow \infty$. The corresponding sequence of reconstructions is given by $\{(-1)^k \frac{1}{k} + (-1)^k \lambda\}_{k \geq 1}$, which does not converge, but has a sub-sequence converging to λ , which is a solution of (5) for $y = 0$.

Imposing (strong) convexity on the regularizer [12] helps achieve stronger forms of convergence

and precludes such discontinuities in the reconstruction. More precisely, for two measurement vectors y_1 and y_2 that are δ apart (in norm on \mathbb{Y}), the corresponding reconstructions can vary (with respect to norm on \mathbb{X}) by at most $\frac{\beta\delta}{\lambda\rho}$, where β is the spectral norm of \mathcal{A} and \mathcal{S}_ρ is ρ -strongly convex. Notably, ACR is also a convergent regularization scheme, meaning that the reconstruction converges to the \mathcal{S}_ρ -minimizing solution of $\mathcal{A}x = y^0$, where y^0 denotes clean data, as the noise level $\delta \rightarrow 0$, provided that the regularization penalty $\delta \mapsto \lambda(\delta)$ satisfies $\lim_{\delta \rightarrow 0} \lambda(\delta) = \lim_{\delta \rightarrow 0} \frac{\delta}{\lambda(\delta)} = 0$. The importance of convexity prior for stability is demonstrated through the example of limited-view CT reconstruction from [12]^b in Fig. 4.

^aThanks to Sebastian Lutz for providing this example

^bThanks in particular to Zakhar Shumaylov for the limited-view CT experiments.

B. Iterative unrolling with fixed-point convergence

The main philosophy behind algorithm unrolling is to construct a DNN architecture by unfolding a fixed number of iterations of an optimization algorithm. Subsequently, different components of the algorithm are replaced by learnable units (typically modeled using shallow networks) and the overall network is trained end-to-end to produce a reconstruction from its corresponding measurement. The origin of unrolling can be traced back to the seminal work by Gregor and LeCun [20] for solving sparse coding via unfolding the iterative soft-thresholding algorithm. The output of the k^{th} layer of a generic unrolled architecture can be expressed as $x_{k+1} = \psi_{\theta_k}(x_k, y)$, where ψ_{θ_k} is a non-linear mapping with parameters θ_k . Unrolled networks, trained with enough expressive power and training data, approximate the conditional mean of the image given its measurement. However, without any further assumptions on ψ_{θ_k} , it is generally not possible to characterize the estimate of an unrolled network as the stationary point of a variational potential or a fixed-point of a non-linear map. Further, one trains an unrolled architecture for a few iterations (typically ≤ 20) due to computational constraints, and the reconstruction deteriorates if more iterations are performed at test time than the number of iterations that were used in training.

This problem was addressed in [21] by using two techniques: (i) weight-sharing, i.e., by using the same set of parameters at each layer ($\theta_k = \theta$ for all k), and (ii) by explicitly constraining the output $x^*(y, \theta)$ of the unrolled network to be a fixed-point of ψ_θ . The training problem reads

$$\min_{\theta} \frac{1}{2} \|x^*(y, \theta) - x\|_2^2 \quad \text{subject to } x^*(y, \theta) = \psi_\theta(x^*(y, \theta), y). \quad (7)$$

It is shown in [21] that the trained map ψ_θ can be applied iteratively beyond the number of iterations trained without any degradation in reconstruction quality. The resulting architectures are referred to as deep equilibrium networks, with fixed-point convergence incorporated into them by construction.

Unrolling an iterative scheme can be constructed to have convergence. The key idea behind such constructions is to parametrize the neural network in a manner such that it corresponds to the proximal

operator of an underlying proper, convex, and lower semi-continuous function. One example is Parseval proximal neural network [22] that use tight frames to parametrize the affine layers.

C. One-step methods

The one-step methods consist in learning a deep neural network-based post-processing of a model-based reconstruction based on pairs of input and target images [4]. More specifically, the reconstruction operator is parameterized as $\mathcal{R}_\theta := \mathcal{C}_\theta \circ \mathcal{B}$, where $\mathcal{B}: \mathbb{Y} \rightarrow \mathbb{X}$ denotes a classical reconstruction method (with no or few tune-able parameters, e.g., FBP or TV in X-ray CT) and $\mathcal{C}_\theta: \mathbb{X} \rightarrow \mathbb{X}$ represents a deep convolutional network with parameters θ . The reconstructed image produced by such a post-processing method fails to satisfy the data-consistency criterion. That is, a small value of $\|\mathcal{A}x^\dagger - y^\delta\|$ does not necessarily imply a small value for the data-fidelity term $\|\mathcal{A}\mathcal{C}_\theta(x^\dagger) - y^\delta\|$ corresponding to the output of \mathcal{C}_θ , where x^\dagger is the reconstruction obtained using \mathcal{B} . Consequently, such post-processing schemes do not lead to convergent regularization strategies. This issue was addressed in [23] by parametrizing the operator \mathcal{C}_θ as $\mathcal{C}_\theta = \text{Id} + (\text{Id} - \mathcal{A}^\dagger \mathcal{A}) \mathcal{Q}_\theta$, where \mathcal{Q}_θ is a Lipschitz-continuous DNN. Since $(\text{Id} - \mathcal{A}^\dagger \mathcal{A})$ is the projection operator on to the null-space of \mathcal{A} , the operator \mathcal{C}_θ (referred to as null-space network) always satisfies $\mathcal{A}\mathcal{C}_\theta(x^\dagger) = \mathcal{A}x^\dagger$, ensuring that the output of \mathcal{C}_θ explains the observed data. Null-space networks are shown to provide convergent regularization schemes [23].

Deep convolutional framelets [5] aim to gain a better understanding and interpretability of deep learning by establishing a link with wavelet theory. An image is here represented by convolving local and non-local bases. The convolutional framelets generalize the theory of low-rank Hankel matrix approaches for inverse problems and [5] extends the idea to obtain a DNN using multilayer convolutional framelets that enable perfect representation of an image. The analysis in [5] shows that the popular deep network components such as residual block, redundant filter channels, and concatenated rectified linear units (ReLU) do indeed offer perfect representation, while the pooling and unpooling layers should be augmented with high-pass branches to meet the perfect representation condition.

D. Plug-and-play denoising

Reconstruction in the variational setting typically requires an iterative algorithm to minimize the underlying variational loss. Popular iterative techniques such as PGD and alternating-directions method of multipliers (ADMM) entail applying the proximal operator corresponding to the (possibly non-smooth) regularizer to update the estimate. The seminal work by Venkatakrisnan et al. [24] pioneered the idea of replacing the proximal operator with an off-the-shelf denoiser. To give a specific example, such a plug-and-play (PnP)-denoising used inside the PGD algorithm leads to the iterative scheme $x_{k+1} = D_\sigma \left(x_k - \eta \nabla_x \mathcal{L}_\mathbb{Y}(\mathcal{A}x, y) \Big|_{x=x_k} \right)$ for reconstruction, starting from an initial estimate x_0 . Here, $D_\sigma: \mathbb{X} \rightarrow \mathbb{X}$ is typically a denoiser to remove Gaussian noise of standard deviation σ . Traditionally,

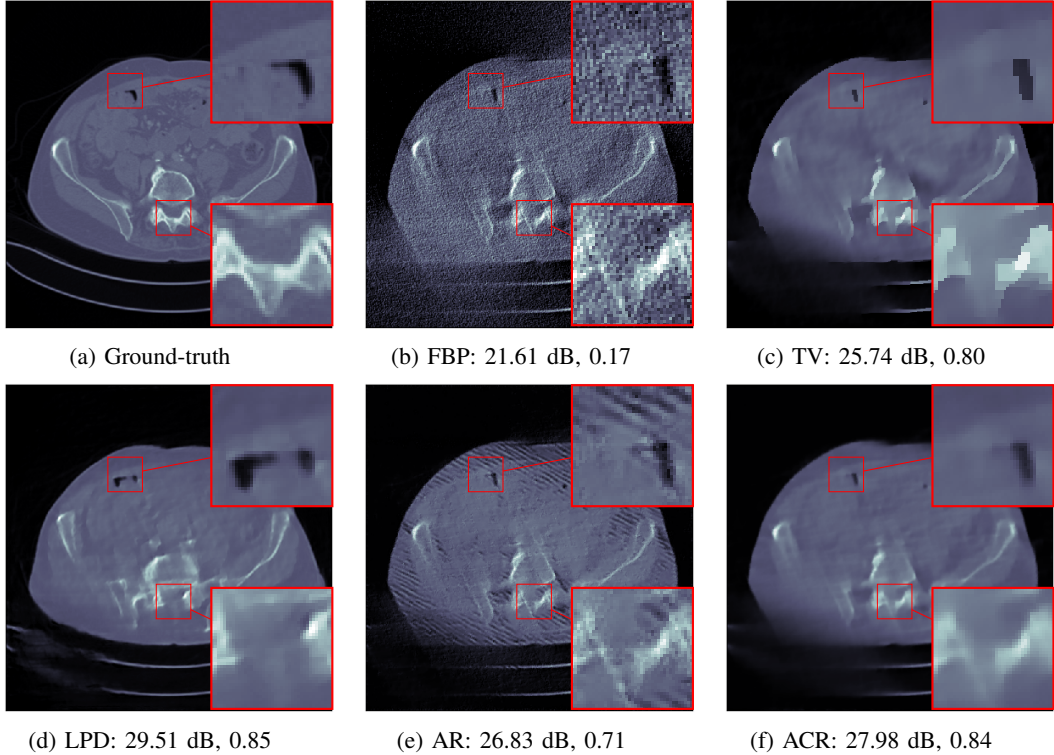


Fig. 4: A comparison of different model-driven and learned methods for limited-angle CT (with the PSNR (dB) and SSIM scores indicated below). While the FBP reconstruction is noisy, TV fails to preserve important details in the reconstructed image. The LPD method, which was trained on pairs of ground-truth images and limited-angle projection data in this case, does not faithfully reconstruct the image, especially the highlighted regions. One possible reason behind this is that LPD, or any other end-to-end supervised method for that matter, does not necessarily produce a data-consistent reconstruction (see Sec. IV-C for further explanation). The AR leads to artifacts in the reconstructed image, as it favors oscillations in the direction of blurring artifacts in the FBP images. Imposing convexity on the regularizer helps prevent such oscillations and resulting instability, as seen in the images reconstructed by ACR. Notably, unlike LPD and AR, ACR is a convergent regularization scheme and the reconstructions exemplify the importance of this type of theoretical guarantee.

the choice of the denoiser has been model-inspired (e.g., BM3D, dictionary-based denoisers like K-SVD, TV, etc.), but more recently, PnP algorithms have used off-the-shelf deep neural network-based denoisers (e.g., DnCNN). These methods have shown excellent empirical performance for practical inverse problems, which inspired a recent line of research to analyze their convergence theoretically. Generally, PnP methods, subject to appropriate conditions on the denoiser, have been shown to possess fixed-point and/or objective convergence.

One of the first results on the global objective convergence of PnP-ADMM was shown in [25]. Their theorem requires that the denoiser is continuously differentiable and has a doubly-stochastic gradient matrix, which are equivalent to the denoiser being a proximal operator for some convex function. Fixed-point convergence of PnP-ADMM with a continuation scheme and bounded denoisers was established in [26]. It was shown in [27] that the iterations of PnP-PGD and PnP-ADMM are contractive (and, hence converges to a fixed-point) if the denoiser satisfies a ‘Lipschitz-like’ condition (see Assumption A in [27]). Both objective and fixed-point convergence of PnP-forward-backward splitting (FBS) and PnP-ADMM were proved in [28] for linear denoisers $D(x) = \mathbf{W}x$, where \mathbf{W} is

diagonalizable with eigenvalues in $[0, 1]$. The denoiser scaling approach, which provides a systemic way to control the regularization of PnP denoisers, is shown to be fixed-point convergent using the consensus equilibrium (CE) framework [29].

Typically, The convergence results for PnP methods either assume the denoiser to satisfy a hard Lipschitz bound, or require the data-fidelity term to be strongly-convex in x . While the former is restrictive for deep denoisers, as it affects the denoising performance adversely, the latter assumption excludes inverse problems where the forward operator has a non-trivial null-space (e.g., in sparse-view CT). Recently, convergence guarantees for PnP methods were derived in [30] for various splitting algorithms with gradient-step (GS) denoisers, alleviating the need for such restrictive assumptions. GS denoisers are constructed as $D_\sigma = \text{Id} - \nabla g_\sigma$, where $g_\sigma(x) = \frac{1}{2} \|x - \mathcal{P}_\sigma(x)\|_2^2$, with \mathcal{P}_σ being a deep network without any structural constraints. This parametrization was shown to have enough expressive power to achieve state-of-the-art denoising performance in [30]. Notably, GS denoisers have a scalar potential given by $h_\sigma(x) = \frac{1}{2} \|x\|_2^2 - g_\sigma(x)$. When the potential h_σ is convex, GS denoisers are proximal operators corresponding to a potentially non-convex function. Therefore, this approach can target to minimize a variational objective with a potentially non-convex regularizer.

A closely related PnP approach was adopted in [31] with a similar aim of providing an asymptotic characterization of iterative PnP solutions. The main idea was to model maximally monotone operators (MMO) using a NN and interpret the reconstruction as the solution of a monotone inclusion problem (which generalizes convex optimization problems). The parametrization of MMOs was done by modeling the resolvent via a non-expansive NN.

Regularization-by-denoising (RED) is another prominent PnP approach that utilizes an off-the-shelf denoiser $D(x)$ to construct an explicit regularizer $\mathcal{S}(x) = x^\top (x - D(x))$. If the denoiser is such that the gradient condition $\nabla \mathcal{S}(x) = x - D(x)$ holds, the RED algorithms recover the stationary point of $x \mapsto \frac{1}{2} \|Ax - y\|_2^2 + \lambda \mathcal{S}(x)$. It was shown in [32] that the gradient condition does not hold for denoisers with a non-symmetric Jacobian, which is the case for most practical (classical or data-driven). A new analysis framework based on score-matching was developed in [32] to explain the empirical success of the RED algorithms. Specifically, if the denoiser is such that $\frac{D(x)-x}{\epsilon}$ approximates the score function (i.e., the gradient of the log prior), the stationarity condition for the MAP estimation problem (with the prior replaced by a smooth surrogate) leads to the following fixed-point equation (see Sec. IV.C in [32]): $\frac{1}{2} \mathcal{A}^\top (\mathcal{A}x^* - y) + \lambda (x^* - D(x^*))$, where $\lambda = \frac{\sigma^2}{\epsilon}$, with σ^2 being the variance of measurement noise. The equation above is identical to the fixed-point equation that the RED algorithm seeks to recover. Here, the denoiser D is not required to have a symmetric Jacobian. With this new interpretation, several variants of the RED algorithm were proposed in [32] with fixed-point convergence.

Objective convergence of PnP with GS denoisers

The convergence of PnP denoisers used with half-quadratic splitting (HQS) was established in [30]. The denoiser is constructed as a GS denoiser as explained in Sec. IV-D, i.e., $D_\sigma = \text{Id} - \nabla g_\sigma$, where g_σ is proper, lower semi-continuous, and differentiable with an L -Lipschitz gradient. The PnP algorithm proposed in [30] takes the form $x_{k+1} = \text{prox}_{\tau f}(x_k - \tau \lambda \nabla g_\sigma(x_k))$, where $f: \mathbb{R}^d \rightarrow \mathbb{R} \cup \{+\infty\}$ measures the data-fidelity and is assumed to be convex and lower semi-continuous. Under these assumptions on f and g_σ , the following guarantees hold for $\tau < \frac{1}{\lambda L}$:

- 1) The sequence $F(x_k)$, where $F = f + \lambda g_\sigma$, is non-increasing and convergent.
- 2) $\|x_{k+1} - x_k\|_2 \rightarrow 0$, which indicates that iterations are stable, in the sense that they do not diverge if one iterates indefinitely.
- 3) All limit points of $\{x_k\}$ are stationary points of $F(x)$.

E. Learned optimization solvers

Reconstruction in imaging inverse problems is framed as an optimization problem as in (1), which could be computationally demanding to solve, especially when the image lives in a high-dimensional vector space. Some recent works [11] have developed data-driven solvers with convergence guarantees for minimizing convex variational objectives. They seek to learn a solver for a family of optimization problems of the form $\min_{x \in \mathbb{X}} F_y(x)$, parametrized by y . In the context of inverse problems, the functional $F_y(x)$ is the variational objective defined in (1). The key idea is to build a parametric solver of the form $\mathcal{T}_{N,\theta}: \mathbb{Y} \rightarrow \mathbb{X}$ by unrolling a fixed number of iterations (denoted as N) of a gradient-based algorithm. Subsequently, the parameters θ of the solver are learned in an unsupervised manner by minimizing $\frac{1}{n} \sum_{i=1}^n F_{y_i}(\mathcal{T}_{N,\theta}(y_i))$ over θ , where $(y_i)_{i=1}^n$ are n i.i.d. samples drawn from the marginal distribution of the data y . The iterative solver is constructed by adding a neural network-based deviation term to the gradient-based update, and convergence is shown in the case where the deviation term lies in an appropriately defined set. In practice, such learned solvers converge significantly faster than a conventional first-order solver with suitably chosen step-size parameters. See Sections 3 and 4 in [11] for more technical details about the construction and convergence proof of learned optimization solvers.

F. Provable Bayesian methods

As mentioned previously, the Bayesian framework represents the unknown image as a random variable \mathbb{x} taking values in \mathbb{X} . The observed data $y \in \mathbb{Y}$ is understood as a realization of an \mathbb{Y} -valued random variable \mathbb{y} , related to \mathbb{x} by the joint probability distribution of (\mathbb{x}, \mathbb{y}) . The latter is usually specified via its joint density function $p(x, y)$ through the decomposition $p(x, y) = p(y|x)p(x)$, where the data likelihood function $p(y|x)$ is derived from the conditional distribution of $(\mathbb{y}|\mathbb{x} = x)$ related to the measurement process, and $p(x)$ is the so-called *prior* density of \mathbb{x} . We focus on Bayesian strategies

that seek to learn the prior for \mathbb{X} from training data $\{x_i\}_{i=1}^n$, which we regard as i.i.d. samples from the true marginal distribution of \mathbb{X} . This is achieved by adopting the so-called M-complete Bayesian modeling paradigm in which there exists a true or *oracle* prior distribution that is decision-theoretically optimal but unknown (represented only by the samples $\{x_i\}_{i=1}^n$), and where we regard all other models as operational approximations of the oracle. For clarity, we assume that the oracle marginal distribution admits a density, henceforth denoted by $p^*(x)$.

By involving the likelihood function $p(y|x)$ and by using Bayes' theorem, we derive an oracle posterior distribution for $(\mathbb{X}|y = y)$ with density $p^*(x|y) = \frac{p(y|x)p^*(x)}{\int_{\mathbb{X}} p(y|\tilde{x})p^*(\tilde{x})d\tilde{x}}$. Unfortunately, this decision-theoretically optimal model is not available in practice. Bayesian strategies to perform inference with priors derived from the training data seek to approximate this oracle posterior in different ways. Here, we focus on theoretically rigorous and provably convergent strategies that encode $\{x_i\}_{i=1}^n$ in the form of a denoising end-to-end neural network that is used in a PnP fashion, and on strategies that rely on a generative model trained to reproduce the distribution of $\{x_i\}_{i=1}^n$.

a) Bayesian methods with PnP priors: Let $D_\sigma^* : \mathbb{X} \mapsto \mathbb{X}$ denote the optimal minimum mean-squared error (MMSE) denoiser to remove Gaussian noise of standard deviation σ from an image taking values in \mathbb{X} according to the prior p^* . In principle, D_σ^* can be derived from p^* by using Bayesian decision theory. In practice, D_σ^* is unknown because p^* is unknown, but it can be approximated by a deep network D_σ trained on samples $\{x_i\}_{i=1}^n$ from p^* . PnP Bayesian methods use a suitably trained denoiser D_σ in order to perform approximate inference w.r.t. the oracle $p^*(x|y)$. This is achieved by using $D_\sigma \approx D_\sigma^*$ to mimic gradient-based Bayesian computation algorithms that target a regularized approximation of $p^*(x|y)$, which, by construction, verifies the regularity properties required for fast convergence [33], [34]. More precisely, PnP Bayesian methods stem from the observation that D_σ^* is related to p^* by Tweedie's identity, i.e., $\sigma^2 \nabla \log p_\sigma^*(x) = D_\sigma^*(x) - x$, for all $x \in \mathbb{X}$ and $\sigma > 0$, where p_σ^* is a regularized approximation of p^* obtained via the convolution of p^* with a Gaussian smoothing kernel of bandwidth σ . Unlike p^* which may be degenerate or non-smooth, p_σ^* is by construction proper and smooth, with its gradient $x \mapsto \nabla \log p_\sigma^*(x)$ being globally Lipschitz continuous under mild conditions on p_σ^* [33]. Also, $p_\sigma^*(x)$ can be made arbitrarily close to $p^*(x)$ by reducing σ .

Equipped with this regularized prior, PnP Bayesian methods use Bayes' theorem to derive the regularized posterior density $p_\sigma^*(x|y) \propto p(y|x)p_\sigma^*(x)$. Under mild assumptions on $p(y|x)$, $p_\sigma^*(x|y)$ inherits the favorable regularity properties of $p_\sigma^*(x)$ and provides an approximation to the oracle $p^*(x|y)$ that is amenable to efficient computation by gradient-based algorithms such as the unadjusted Langevin algorithm (ULA) and stochastic gradient descent (SGD) [33]. Moreover, through σ , the approximation $p_\sigma^*(x|y)$ can be made as close to $p^*(x|y)$ as required in order to control the estimation bias, at the expense of additional computational effort because of slower convergence of gradient-based algorithms. In addition, [33] provides verifiable conditions that guarantee that $p_\sigma^*(x|y)$ and key quantities such as

posterior moments exist and are stable w.r.t. the observed data y .

The main theoretical insight underpinning PnP Bayesian methods such as the PnP-ULA and PnP-SGD studied in [33], [34] is that one can use $\nabla \log p_\sigma^*$ to formulate idealized ULA and SGD algorithms for inference w.r.t. p_σ^* , and subsequently substitute $\nabla \log p_\sigma^*(x) = (D_\sigma^*(x) - x)/\sigma^2$ within these algorithms by $(D_\sigma(x) - x)/\sigma^2$ without significantly perturbing their convergence properties, even if $D_\sigma(x)$ is not a gradient or an MMO. Approximating D_σ^* by D_σ introduces some bias; i.e., the algorithms deliver a solution in the neighborhood of the oracle solution that would be produced by the idealized algorithms. The magnitude of this bias w.r.t. the oracle depends primarily on how close D_σ is to D_σ^* .

We are now in a position to introduce PnP-ULA for Monte Carlo (MC) sampling and MMSE estimation, as well as PnP-SGD for MAP estimation. Let $C \subset \mathbb{X}$ denote a compact convex set that contains most of the prior probability mass of \mathbb{x} . PnP-ULA is defined by following recursion [33]: given an initial state $x_0 \in \mathbb{X}$ and for any $k \in \mathbb{N}$

$$x_{k+1} = x_k + \delta \nabla \log p(y|x_k) + \frac{\delta}{\sigma^2} [D_\sigma(x_k) - x_k] + \frac{\delta}{\lambda} [\Pi_C(x_k) - x_k] + \sqrt{2\delta} z_{k+1}, \quad (8)$$

where Π_C is the projection operator onto C , $\{z_k\}_{k \in \mathbb{N}}$ are i.i.d. standard Gaussian random variables, $\lambda > 0$ is a tail regularization parameter that is set such that PnP-ULA converges to its target density geometrically fast, and $\delta > 0$ is a step-size that trades-off asymptotic accuracy with convergence speed.

Under suitable conditions on δ and λ , the sequence generated by PnP-ULA is a Markov chain which converges geometrically fast to an approximation of $p_\sigma^*(x|y)$ whose accuracy depends explicitly on the number of iterations of PnP-ULA, $\|D_\sigma - D_\sigma^*\|$, and on the values of δ , λ , C , and X_0 . Convergence holds in the TV-norm, as well as in the Wasserstein-1 norm, guaranteeing the convergence of MC estimators for probabilities, the posterior mean and posterior covariance. We refer the reader to [33] for details and for a variant of PnP-ULA for problems involving hard constraints. Note that in problems where the forward operator \mathcal{A} is random and right-rotationally invariant, it is possible to perform approximate point estimation for $(\mathbb{x}|y = y)$ very efficiently by using the approximate message passing (AMP) algorithm of [35], which is provably convergent in a certain large system limit.

With regards to MAP estimation for $p_\sigma^*(x|y)$, i.e. $\hat{x}_{\text{map}} \in \arg \max_{x \in \mathbb{X}} p_\sigma^*(x|y)$, it is worth mentioning two main results from [34] before discussing computation. First, MAP solutions of $p_\sigma^*(x|y)$ lie in a neighborhood of MAP solutions of $p^*(x|y)$ and they vary in a stable manner w.r.t. σ , with the two sets of solutions coinciding as $\sigma \rightarrow 0$. Second, MAP solutions of $p_\sigma^*(x|y)$ are locally Lipschitz continuous w.r.t. to perturbations in $y \in \mathbb{Y}$, which is a mild form of well-posedness (see [34] for details).

For computation, we consider the PnP-SGD algorithm defined by the following recursion [34]: given an initial state $x_0 \in \mathbb{X}$ and for any $k \in \mathbb{N}$

$$x_{k+1} = x_k + \delta_k \nabla \log p(y|x_k) + \frac{\delta_k}{\sigma^2} [D_\sigma(x_k) - x_k] + \delta_k z_{k+1}, \quad (9)$$

where $\{\delta_k\}_{k \in \mathbb{N}}$ is a family of decreasing positive step-sizes and $\{z_k\}_{k \in \mathbb{N}}$ are again i.i.d. standard Gaussian random variables. Proposition 3 of [34] states that stable PnP-SGD sequences converge close to stationary points of $\nabla \log p_\sigma(x|y)$, with an accuracy that depends on $\|D_\sigma - D_\sigma^*\|$.

For illustration, Fig. 5 presents the results of an image deblurring experiment from [33] where PnP-ULA and PnP-SGD are used to compute the MMSE and MAP estimators, using the denoiser of [27] with $\sigma = 5/255$. A main strength of MC algorithms such as PnP-ULA is their capacity for Bayesian analyses beyond point estimation, such as uncertainty quantification (bottom row in Fig. 5).

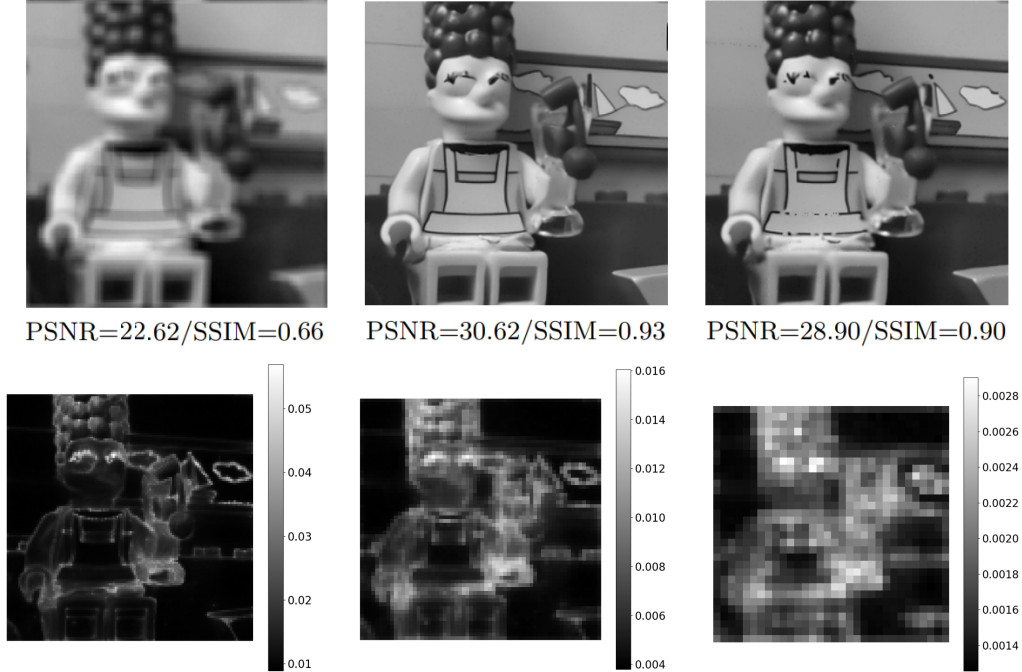


Fig. 5: Image deblurring using the denoiser [27] in a PnP fashion. Top row shows data (left), a blurred 256×256 image with additive Gaussian noise with standard deviation $1/255$, along with MMSE solution from PnP-ULA (middle) and MAP solution from PnP-SGD (right). Bottom row shows uncertainty plots at the scales of 2×2 (left), 4×4 (middle), and 8×8 pixels (right), computed by PnP-ULA. See [33] for details.

b) Bayesian methods with generative priors: In this case, one seeks to construct a prior distribution for \mathbb{x} by using the training data $\{x_i\}_{i=1}^n$ and by leveraging recent developments in deep generative modeling, such as VAEs, GANs, and normalizing flows. We first discuss the Bayesian method of [36] which adopts the manifold hypothesis to construct a prior distribution for \mathbb{x} that is supported on a sub-manifold of \mathbb{X} of dimension much smaller than \mathbb{X} . Operating on this manifold of dramatically reduced dimensionality simultaneously allows to effectively regularize ($\mathbb{x}|y = y$) and to perform computations efficiently. In [36], this is achieved by introducing a latent Gaussian variable $z \sim \mathcal{N}(0, \mathbb{I}_d)$ on \mathbb{R}^d and a deep network $\mathcal{T}_\theta: \mathbb{R}^d \mapsto \mathbb{X}$ designed such that $\mathcal{T}_\theta(z)$ for $z \sim \mathcal{N}(0, \mathbb{I}_d)$ is close to $\{x_i\}_{i=1}^n$ (e.g., by using a VAE architecture). Given this construction, [36] derives the latent posterior distribution $p(z|y) \propto p(y|z)p(z)$, where $p(z)$ is a standard Gaussian density on \mathbb{R}^d and the likelihood is $p(y|z) = p_{y|\mathbb{x}}(y|\mathcal{T}_\theta(z))$. The posterior distribution of ($\mathbb{x}|y = y$) is then given by using \mathcal{T}_θ to map ($z|y = y$) onto \mathbb{X} . The Bayesian inverse problem is shown to be well-posed for ($z|y = y$) and

$(\mathbb{x}|\mathbb{y} = y)$ under mild conditions on the likelihood, and key quantities such as the posterior mean exist.

With regards to computation, [36] adopts a preconditioned Crank-Nicolson MCMC algorithm targeting $p(z|y)$, which is provably ergodic under realistic and easily verifiable conditions. MC samples for $(\mathbb{x}|\mathbb{y} = y)$ are then obtained by using \mathcal{T}_θ to project the sample from $(z|\mathbb{y} = y)$ onto \mathbb{X} . One can also perform approximate MMSE or MAP estimation for $(z|\mathbb{y} = y)$ efficiently by using the AMP algorithms of [37], which converge to the true MMSE or MAP solutions in a certain large system limit.

Furthermore, [38] also considers a Bayesian model with a prior encoded by a VAE, with a focus on MAP estimation. Unlike [36] that constraints \mathbb{x} to take values on the range of \mathcal{T}_θ in order to reduce dimensionality, [38] considers an augmented model $p(x, z)$ on $\mathbb{X} \times \mathbb{R}^d$ that concentrates mass in the neighborhood of $x = \mathcal{T}_\theta(z)$ while carefully allowing for deviations from this sub-manifold to better fit the training images. This leads to an augmented posterior distribution $p(x, z|y) \propto p(y|x)p(x, z)$ that is a more accurate model than the marginal posterior model considered in [36]. Inference with $p(x, z|y)$ is significantly more computationally challenging, a difficulty that [38] addresses by focusing exclusively on MAP estimation. Crucially, the authors establish that the potential $(x, z) \mapsto -\log p(x, z|y)$ is weakly bi-convex under realistic conditions on the VAE, and subsequently propose three provably convergence alternating optimization schemes to compute a critical point of this potential efficiently.

V. CONCLUSIONS AND OUTLOOK

In scientific disciplines where imaging drives new discoveries or in real-world applications where imaging is used for making critical decisions, it is essential to have mathematical correctness guarantees for the algorithms used for image recovery. While the classical variational approaches come with such certificates, they fall short in terms of empirical performance as compared to the modern data-driven imaging algorithms. We formalized different notions of correctness as it applies to image reconstruction methods and surveyed some of the notable deep learning-based approaches, both deterministic and stochastic, that fit within these notions. We discussed some of the essential components, e.g., network architecture design, training strategies, etc. that typically aid deriving such theoretical certificates. While we sought to dispel the widely held belief about the black-box nature of deep learning algorithms for image reconstruction, we also highlighted the gaps in theoretical understanding about well-performing methods rooted in robust heuristics. The methods we reviewed in this article broadly derive their origin from the variational regularization framework and convex analysis, two of the major theoretical pillars that the classical methods rest on. In fact, convexity arose as a recurring theme for proving convergence results in both deterministic and stochastic settings, which underscores the importance of ICNNs for combining classical theory with data-driven learning. In summary, we argued that the classical mathematical machinery can go a long way when it comes to devising and analyzing data-driven methods, leading to better reliability and transparency of deep learning for imaging.

REFERENCES

- [1] M. Benning and M. Burger, “Modern regularization methods for inverse problems,” *Acta Numerica*, vol. 27, pp. 1–111, 2018.
- [2] S. Arridge, P. Maass, O. Öktem, and C.-B. Schönlieb, “Solving inverse problems using data-driven models,” *Acta Numerica*, vol. 28, pp. 1–174, 2019.
- [3] M. Pereyra, “Revisiting maximum-a-posteriori estimation in log-concave models,” *SIAM Journal on Imaging Sciences*, vol. 12, pp. 650–670, 01 2019.
- [4] K. H. Jin, M. T. McCann, E. Froustey, and M. Unser, “Deep convolutional neural network for inverse problems in imaging,” *IEEE Transactions on Image Processing*, vol. 26, no. 9, pp. 4509–4522, 2017.
- [5] J. C. Ye, Y. Han, and E. Cha, “Deep convolutional framelets: A general deep learning framework for inverse problems,” *SIAM Journal on Imaging Sciences*, vol. 11, no. 2, pp. 991–1048, 2018.
- [6] J. Adler and O. Öktem, “Learned primal-dual reconstruction,” *IEEE Transactions on Medical Imaging*, vol. 37, no. 6, pp. 1322–1332, 2018.
- [7] K. Hammernik *et al.*, “Learning a variational network for reconstruction of accelerated MRI data,” *Magnetic Resonance in Medicine*, vol. 79, no. 6, pp. 3055–3071, 2018.
- [8] A. Bora, A. Jalal, E. Price, and A. G. Dimakis, “Compressed sensing using generative models,” in *Proceedings of Machine Learning Research*, vol. 70, 2017, proceedings of the 34th International Conference on Machine Learning, Sydney, Australia.
- [9] H. Li, J. Schwab, S. Antholzer, and M. Haltmeier, “NETT: solving inverse problems with deep neural networks,” *Inverse Problems*, vol. 36, no. 6, 2020.
- [10] S. Lunz, O. Öktem, and C.-B. Schönlieb, “Adversarial regularizers in inverse problems,” in *32nd Conference on Neural Information Processing Systems (NeurIPS 2018)*, Montréal, Canada, 2018, pp. 8507–8516.
- [11] S. Banert, J. Rudzusika, O. Öktem, and J. Adler, “Accelerated forward-backward optimization using deep learning,” *arXiv:2105.05210v1*, 2021.
- [12] S. Mukherjee *et al.*, “Learned convex regularizers for inverse problems,” *arXiv:2008.02839v2*, 2020.
- [13] M. Genzel, J. Macdonald, and M. Marz, “Solving inverse problems with deep neural networks - robustness included,” *IEEE Transactions on Pattern Analysis and Machine Intelligence*, pp. 1–1, 2022.
- [14] A. L. Gibbs and F. E. Su, “On choosing and bounding probability metrics,” *International Statistical Review / Revue Internationale de Statistique*, vol. 70, no. 3, pp. 419–435, 2002. [Online]. Available: <http://www.jstor.org/stable/1403865>
- [15] B. Amos, L. Xu, and J. Z. Kolter, “Input convex neural networks,” in *International Conference on Machine Learning*, 2017, pp. 146–155.
- [16] A. Habring and M. Holler, “A generative variational model for inverse problems in imaging,” *SIAM J. Mathematics of Data Science*, vol. 4, no. 1, pp. 306–335, 2022.
- [17] D. Ulyanov, A. Vedaldi, and V. Lempitsky, “Deep image prior,” in *Proceedings of the IEEE Conference on Computer Vision and Pattern Recognition*, 2018, pp. 9446–9454.
- [18] G. Jagatap and C. Hegde, “Algorithmic guarantees for inverse imaging with untrained network priors,” in *33rd Conference on Neural Information Processing Systems (NeurIPS 2019)*, Vancouver, Canada, 2019.
- [19] A. Raj, Y. Li, and Y. Bresler, “GAN-based projector for faster recovery in compressed sensing with convergence guarantees,” in *2019 IEEE/CVF International Conference on Computer Vision (ICCV)*, 2019.
- [20] K. Gregor and Y. LeCun, “Learning fast approximations of sparse coding,” in *Intl. Conf. on Machine Learning*, 2010.
- [21] D. Gilton, G. Ongie, and R. Willett, “Deep equilibrium architectures for inverse problems in imaging,” *IEEE Transactions on Computational Imaging*, vol. 7, pp. 1123–1133, 2021.
- [22] M. Hasannasab *et al.*, “Parseval proximal neural networks,” *Journal of Fourier Analysis and Applications*, vol. 26, no. 4, Jul. 2020.
- [23] J. Schwab, S. Antholzer, and M. Haltmeier, “Deep null space learning for inverse problems: convergence analysis and rates,” *Inverse Problems*, vol. 35, no. 2, p. 025008, 2019.

- [24] S. V. Venkatakrishnan, C. A. Bouman, and B. Wohlberg, "Plug-and-play priors for model based reconstruction," in *2013 IEEE Global Conference on Signal and Information Processing*, 2013, pp. 945–948.
- [25] S. Sreehari *et al.*, "Plug-and-play priors for bright field electron tomography and sparse interpolation," *IEEE Transactions on Computational Imaging*, vol. 2, no. 4, pp. 408–423, 2016.
- [26] S. H. Chan, X. Wang, and O. A. Elgandy, "Plug-and-play ADMM for image restoration: Fixed-point convergence and applications," *IEEE Transactions on Computational Imaging*, vol. 3, no. 1, pp. 84–98, 2017.
- [27] E. Ryu *et al.*, "Plug-and-play methods provably converge with properly trained denoisers," in *Proceedings of the 36th International Conference on Machine Learning*, vol. 97. PMLR, 09–15 Jun 2019, pp. 5546–5557.
- [28] P. Nair, R. G. Gavaskar, and K. N. Chaudhury, "Fixed-point and objective convergence of plug-and-play algorithms," *IEEE Transactions on Computational Imaging*, vol. 7, pp. 337–348, 2021.
- [29] X. Xu *et al.*, "Boosting the performance of plug-and-play priors via denoiser scaling," in *54th Asilomar Conference on Signals, Systems, and Computers*, 2020, pp. 1305–1312.
- [30] S. Hurault, A. Leclaire, and N. Papadakis, "Gradient step denoiser for convergent plug-and-play," *CoRR*, vol. abs/2110.03220, 2021. [Online]. Available: <https://arxiv.org/abs/2110.03220>
- [31] J.-C. Pesquet, A. Repetti, M. Terris, and Y. Wiaux, "Learning maximally monotone operators for image recovery," *SIAM Journal on Imaging Sciences*, vol. 14, no. 3, pp. 1206–1237, 2021.
- [32] E. T. Reehorst and P. Schniter, "Regularization by denoising: clarifications and new interpretations," *IEEE Transactions on Computational Imaging*, vol. 5, no. 1, pp. 52–67, 2019.
- [33] R. Laumont *et al.*, "Bayesian imaging using plug and play priors: when Langevin meets Tweedie," *SIAM J. Imaging Sciences*, 2021, to appear.
- [34] —, "On Maximum-a-Posteriori estimation with Plug and Play priors and stochastic gradient descent," *HAL preprint hal-0334873*, 2021.
- [35] A. K. Fletcher *et al.*, "Plug in estimation in high dimensional linear inverse problems a rigorous analysis," *Journal of Statistical Mechanics: Theory and Experiment*, vol. 2019, no. 12, p. 124021, 2019.
- [36] M. Holden, M. Pereyra, and K. C. Zygalakis, "Bayesian imaging with data-driven priors encoded by neural networks: Theory, methods, and algorithms," *SIAM J. Imaging Sciences*, 2021, to appear.
- [37] P. Pandit *et al.*, "Inference with deep generative priors in high dimensions," *IEEE Journal on Selected Areas in Information Theory*, vol. 1, pp. 336–347, 2020.
- [38] M. González, A. Almansa, and P. Tan, "Solving inverse problems by joint posterior maximization with autoencoding prior," *arXiv:2103.01648v3*, 2021.